Experimental investigation of slow-positron emission from 4H-SiC and 6H-SiC surfaces

2002 J. Phys.: Condens. Matter 14 6373

(http://iopscience.iop.org/0953-8984/14/25/306)

INSTITUTE OF PHYSICS PUBLISHING JOURNAL OF PHYSICS: CONDENSED MATTER

J. Phys.: Condens. Matter **14** (2002) 6373–6381 PII: S0953-8984(02)33796-2

Experimental investigation of slow-positron emission from 4H-SiC and 6H-SiC surfaces

C C Ling[1], H M Weng[2], C D Beling[1] and S Fung[1]

[1] Department of Physics, The University of Hong Kong, Pokfulam Road, Hong Kong, China
[2] Department of Modern Physics, University of Science and Technology of China, Hefei 230027, China

E-mail: ccling@hkucc.hku.hk

Received 13 February 2002, in final form 17 May 2002
Published 14 June 2002
Online at stacks.iop.org/JPhysCM/14/6373

Abstract

Slow-positron emission from the surfaces of as-grown n-type 4H-SiC and 6H-SiC (silicon carbide) with a conversion efficiency of $\sim 10^{-4}$ has been observed. After 30 min of 1000 °C annealing in forming gas, the conversion efficiency of the n-type 6H-SiC sample was observed to be enhanced by 75% to 1.9×10^{-4}, but it then dropped to $\sim 10^{-5}$ upon a further 30 min annealing at 1400 °C. The positron work function of the n-type 6H-SiC was found to increase by 29% upon 1000 °C annealing. For both p-type 4H-SiC and p-type 6H-SiC materials, the conversion efficiency was of the order of $\sim 10^{-5}$, some ten times lower than that for the n-type materials. This was attributed to the band bending at the p-type material surface which caused positrons to drift away from the positron emitting surface.

1. Introduction

Monoenergetic positron beams have been extensively used in many fields of scientific research such as atomic physics, condensed matter physics and materials sciences [1, 2]. In order to obtain low-energy positrons (several electron volts) with narrow energy distribution, fast positrons originated from a radioactive isotope undergoing a β^+-decay or from a pair production process are moderated by a material having a negative positron work function. The positron work function ϕ_+ can be written as $\phi_+ = -D - \mu_+$, where μ_+ is the positron chemical potential and D is the magnitude of the surface dipole, which is repulsive for the positron [1, 2]. As the energetic positrons enter the moderator, they rapidly thermalize within <10 ps and then undergo diffusion. A fraction of the diffusing positrons may arrive at the surface and will emit into the vacuum if the positron work function of the moderator surface is negative.

Since the first observation of positron emission in vacuum reported by Cherry [3], much effort have been made in the past 40 years to improve moderator conversion efficiency which, in the case of solid Ne, has improved to a value of 7×10^{-3} [4]. Tungsten (W) is, however, the most

commonly used moderator because of its general stability and relatively high efficiency $\sim 10^{-3}$ under non-UHV conditions [2]. In recent years, positron emission has been observed from the surfaces of various wide-band-gap semiconductors (for example, GaN [5, 6], SiC [5–9] and diamond [10]). These wide-band-gap materials having a high electron mobility and a negative positron work function are potential substrate materials for fabricating field-assisted (FA) moderators in which an internal electric field present in the moderator causes the implanted positrons to drift to the emitting surface [11]. One FA moderator system involving dipoles in a rare-gas solid has been achieved by Merrison *et al* [12]. Beling *et al* [13] proposed another FA moderator fabrication technique involving a structure composed of an epitaxial contact on a semiconductor substrate. Observing that a fraction of about 10% of the implanted fast positrons drifted back to the contact of a 200 V negatively biased metal/semi-insulating (SI) GaAs structure, Shan *et al* [14] discussed the possibility of using the metal/SI-GaAs structure as a FA moderator. The greatest difficulty in fabricating a workable metal–semiconductor FA moderator lies in the metal–semiconductor interface which contains vacancy and open-volume trapping defects and presents an unfavourable barrier to positron transmission.

Silicon carbide is a favoured candidate for use as a FA moderator substrate [7, 15]. Room temperature positron diffusion lengths of ∼40–80 nm [7, 8, 16–18] were observed for Lely-grown bulk materials. For the case of epitaxial materials, at room temperature, the positron diffusion length was reported as 348 nm [19] and 250 nm [20] (calculated from the measured values of $D_{eff} \sim 3.5$ cm^2 s^{-1} and $\tau_{ave} \sim 180$ ps in [20]). The n-type SiC materials are also known to emit positrons with energies in the 2.1–3.0 eV range [5–9]. The breakdown electric field of this material is as high as 2×10^6 V cm^{-1} [21] and can probably sustain a positron velocity of $\sim 10^7$ cm s^{-1} before electrical breakdown occurs—similar to the electron saturated velocity [21]. This is encouraging since, with a bulk lifetime of ∼145 ps [22], the positron can drift a distance of ∼10 μm. With an implantation depth of ∼60 μm for ^{22}Na primary positrons, this is equivalent to an efficiency of over 10%.

Unlike previous positron re-emission measurements on SiC which employed monoenergetic slow positrons [5, 7–9], in this study, the samples under investigation were employed as moderators while implanted with energetic positrons from a ^{22}Na radioactive source. The positron work function and the positron emission efficiency are measured on different SiC samples so as to investigate the effect of doping, polytype and annealing.

2. Experimental details

The details of the positron beam facility used in the present study can be found in [6]. The schematic beam diagram in [6] is also included here as figure 1. It consists of a 125 μCi ^{22}Na radioactive source deposited at the tip of a Mo rod implanting fast positrons in reflection geometry at an angle of 20° towards the moderator surface under test. The moderator was held at a positive bias of $+V_a$ relative to an earthed grid in order to accelerate the emitted slow positrons. The slow positrons were guided to the retarding field analyser (RFA) by the longitudinal magnetic field provided by three external field coils. The RFA consisted of a pair of retarding grids biased at V_R so as to decelerate the incidence slow positrons. Another grid biased at $-V_{in}$ relative to the retarding grid was placed after the retarding grids so that positrons had sufficient impact energy for channel electron multiplier (CEM) operation. Emitted positrons having sufficient energy to overcome the potential barrier set up by the RFA would be detected by the CEM. The emission measurements were performed at a vacuum of 10^{-7} Torr.

The SiC samples were cut from Lely-grown Al-doped (p-type) and N-doped (n-type) wafers purchased from Cree Inc. The surface orientations of the 4H-SiC and 6H-SiC substrates were respectively 8.0° and 3.5° towards [11$\bar{2}$0] and the surfaces were all polished Si faces. All

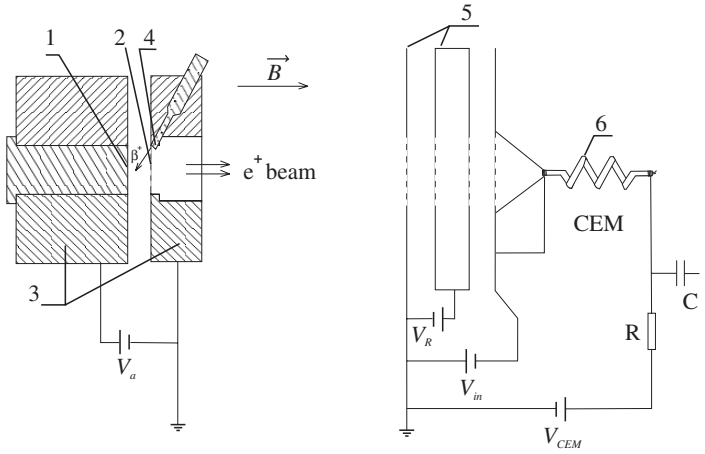

Figure 1. A schematic diagram of the compact monoenergetic positron beam. (1) Moderator sample; (2) extracting and accelerating grid; (3) stainless steel rings; (4) radioactive source (^{22}Na); (5) retarding grids; (6) CEM.

the samples were degreased with acetone and ethanol, and then rinsed with deionized water. The annealing of each sample moderator lasted 30 min and was carried out in a forming gas (N_2:H_2 80:20%) furnace. Following annealing and before exposure to air, the sample was moved into a room temperature region and remained in the forming gas atmosphere while cooling.

In order to measure the positron emission efficiency, the CEM positron detection efficiency had to be found first. This calibration was performed with a ^{22}Na calibrated standard radioactive source and a collimated NaI(Tl) detector placed beside the CEM. The real rate of positrons reaching the CEM was found by measuring the number of 511 keV gamma photons detected by the collimated NaI(Tl) detector. By comparing the number of positrons arriving at the CEM and that detected electronically by the CEM system, the positron detection efficiency of the CEM detection system was determined as 23.5%. The rate of slow-positron detection by the CEM was in the range of about 10 s^{-1} (for the poorly moderating p-type SiC materials) to about 150 s^{-1} (for the n-type SiC materials, which are good moderators).

3. Results and discussion

The rate of positron event detection by the CEM for the as-grown n-type 4H-SiC is plotted against retarding bias V_R (i.e. the integral energy spectrum I) in figure 2(a). The data have been subjected to background subtraction and have been normalized to give a maximum integral count of one. This sigmoidal shape spectrum is typical of the integral energy spectra of samples that emit positrons with a negative work function. As seen in the $I(V_R)$ spectrum, the positron count stays constant while V_R is smaller than about 19 V, and then decreases in the region 19 V $< V_R <$ 23 V, while the positron count stays at the background value as V_R when larger than 23 V.

Referring to figure 1, the emitted positrons having a longitudinal kinetic energy E_z (i.e. parallel to the magnetic field) larger than the pass energy $E_{pass} = eV_R - eV_a - (\phi_g^- - \phi_S^-)$ can reach the CEM, where V_a is the accelerating potential in front of the moderator and $\phi_g - \phi_S$ is the electron contact potential difference between the RFA and the sample [23, 24]. The zero

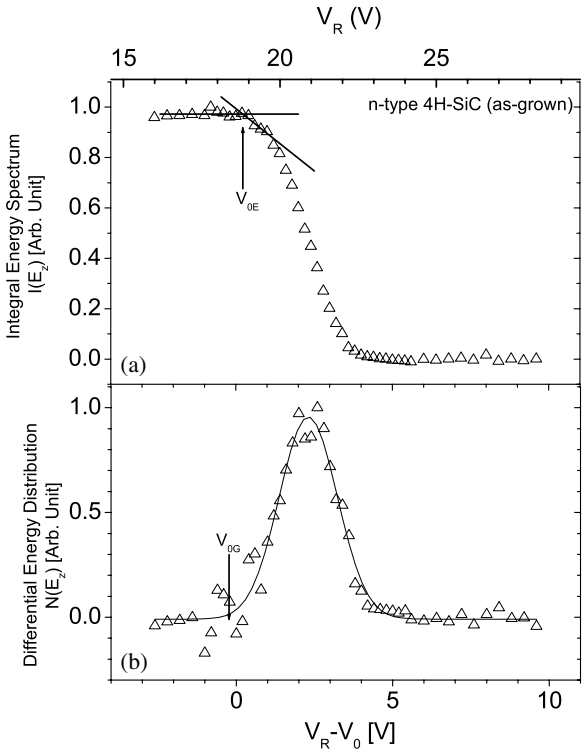

Figure 2. (a) The integral energy spectrum for positrons emitted from as-grown n-type 4H-SiC. (b) The energy distribution of the emitted positrons obtained from differentiating the integral re-emission spectrum in (a). The solid curve is the Gaussian curve fitted to the data.

potential $V_R = V_0$ corresponds to $E_{pass} = 0$ and also to the situation such that the potential difference between the sample and the RFA is zero. With $V_R < V_0$, all emitted positrons can reach the CEM. However, when $V_R > V_0$, only those emitted positrons having longitudinal kinetic energy $E_Z > E_{pass}$ ($=e[V_R - V_0]$) can reach the CEM and this explains the fall-off in integral positron counts as seen in figure 2. As V_R increases further, a condition is finally reached where none of the emitted slow positrons has sufficient energy to cross the potential barrier and thus the positron count drops to zero (or in reality some quiescent background value).

The measured integral energy spectrum $I(V_R)$ is in fact the integral of the differential energy distribution of the emitted positrons $N(E_z)$: $I(E_z) = \int_{E_{pass}}^{\infty} N(E_z)\,\mathrm{d}E_z$. The differential energy distribution $N(E_z)$ for the as-grown n-type 4H-SiC data was obtained by taking the negative derivative of the integral spectrum $I(E_z)$ data and is shown in figure 2(b). As can be seen from the solid curve in figure 2(b), the distribution is fitted very well with a Gaussian function. The peak of the differential energy distribution was $V_{peak} = 20.90 \pm 0.03$ V. We have attempted to work out the zero potential V_0 of the n-type 4H-SiC measurement by two different methods. The first one involves locating the V_0-position by finding the position at which the fitted Gaussian curve drops to $1/100$ of the peak intensity and it was found that $V_{0,G} = 18.3 \pm 0.1$ V. The second method was to locate the V_0-position by extrapolating the falling edge as shown in figure 2(a). Using this method, a value of $V_R = V_{0,E} = 18.9 \pm 0.2$ V was found. As found for the remaining moderator samples, the V_0-value obtained by the

extrapolation method is about 0.3–0.7 V larger than that obtained by the Gaussian fitting method. With the difference between the values of each method being small, it was decided to take the average of the two values; in this case the final $V_0 = 18.6 \pm 0.3$ V. In order to have a clearer picture, an axis giving $V_R - V_0$, which is the longitudinal re-emitted energy, was added in figure 2. The positron work function can be found from the relation $\phi_+ = V_0 - V_{peak}$—that is, the position of the peak of the differential energy spectrum as plotted against $V_R - V_0$. The positron work function of the as-grown 4H-SiC is found to be $\phi_+ = -2.3 \pm 0.5$ eV, where the error comes mainly from the uncertainty of the V_0-position derived from the two methods mentioned.

In addition to the positron work function, the conversion efficiency ε is also found, from the equation: $N_{slow-emit}/N_{fast}$, where $N_{slow-emit}$ and N_{fast} are the number of positrons emitted from the surface and the number of primary fast positrons from the radioactive source. The efficiency so defined is indeed the total efficiency, which includes the source construction effect, the geometric effect, and the quality of the moderator samples. The efficiency of as-grown n-type 4H-SiC was found to be $\varepsilon = 1.3 \pm 0.1 \times 10^{-4}$.

For the case of n-type 6H-SiC materials, positron emission measurements have been performed on the as-grown samples annealed at 650 and 1000 °C. The zero potentials V_0 and the conversion efficiencies ε for each of the measurements were found and these are tabulated in table 1. The conversion efficiencies of each of the samples with slightly different sizes were normalized to the size of 8 mm × 8 mm by considering the solid angle subtended by the sample at the source. It was observed that the efficiency of the N-doped 6H-SiC samples was of the order of $\sim 10^{-4}$ and that there was an increase of 75% as the sample was annealed to 1000 °C in forming gas. With the sample further annealed up to 1400 °C, the conversion efficiency was observed to drop significantly to $\sim 10^{-5}$. It is worth pointing out that, as in the present study, high-energy positrons from the source were implanting into the moderator with a poor source–moderator geometry making an angle of 20° to the moderator surface, and the samples used were Lely-grown bulk material which has positron diffusion lengths of typically several tens of nanometres. This implies that the conversion efficiency can be further increased by improving the source–moderator geometry or using an epitaxial film sample, in which the diffusion length may reach 250–350 nm [19, 20].

As the emission efficiency is given by

$$\varepsilon = G y_0 L_{eff}/R, \tag{1}$$

where G is the geometric factor, y_0 is the branching ratio for positron emission from the surface, and R is the mean implantation depth of the fast positrons. $L_{eff} = \sqrt{D_+ \tau_{eff}}$ is the effective positron diffusion length, where D_+ is the positron diffusion coefficient and τ_{eff} is the average positron lifetime of the sample. Positron lifetime measurements were performed on samples cut from the same wafer and the positron average lifetime for the as-grown and the 900 °C annealed samples were observed to be 164 and 205 ps respectively [19]. The change of the average lifetime was attributed to the annealing-out of silicon and carbon vacancies. These positron traps stop the diffusing positrons from returning to the emitting surface and thus their elimination would lead to an increase of the conversion efficiency. However, from equation (1), the fractional change of the conversion efficiency is related to that of the average positron lifetime by $\Delta\varepsilon/\varepsilon = (1/2)(\Delta\tau_{ave}/\tau_{ave})$. After the annealing, the fractional change of the average positron lifetime is $\Delta\tau_{ave}/\tau_{ave} \sim 25\%$, which is much smaller than the observed fractional change of the conversion efficiency ($\sim$75%). This implies that the drastic increase of the conversion efficiency upon 1000 °C annealing is not predominantly due to the elimination of positron trapping centres, but is mainly due to the change in surface conditions.

Auger electron spectroscopy (AES) was employed to study the difference in chemical

Table 1. Parameters of positron re-emission from different surfaces.

		Zero potential		Fitted Gaussian peak V_{peak} (±0.01 V)	FWHM of the fitted Gaussian (eV)	χ^2 for the Gaussian fit	Positron work function $-\phi_+$ (eV)	Conversion efficiency ε ($\times 10^{-4}$)[a]
		$V_{0,G}$	$V_{0,I}$					
Lely-grown n-type 4H-SiC	As grown	18.3 ± 0.1	18.9 ± 0.2	20.9	2.2	0.96	2.3 ± 0.5	1.3 ± 0.1
Lely-grown n-type 6H-SiC	As grown	18.5 ± 0.1	19.2 ± 0.1	21.0	2.0	0.95	−2.2 ± 0.5	1.1 ± 0.1
	650 °C annealed	18.3 ± 0.1	18.6 ± 0.1	21.0	2.2	0.80	−2.6 ± 0.3	1.0 ± 0.1
	1000 °C annealed	20.3 ± 0.1	20.7 ± 0.2	23.2	2.4	0.91	−2.7 ± 0.4	1.9 ± 0.1
	1400 °C annealed							0.29 ± 0.03
Lely-grown p-type 4H-SiC	As-grown							0.13 ± 0.03
Lely-grown p-type 6H-SiC	As-grown							0.16 ± 0.03
	650 °C annealed							0.13 ± 0.03
	1000 °C annealed							0.16 ± 0.03

[a] The conversion efficiencies were normalized to a sample size of 8 mm × 8 mm.

composition of the surface (first few atomic layers) between the as-grown and the 1000 °C annealed 6H-SiC sample, for which the conversion efficiency was 75% enhanced. The Si (LVV), the C (KVV), and the O (KVV) signals were identified in the differential AES spectra. After the 1000 °C annealing in the forming gas (N_2:H_2 80:20%), the positron emitting surface of the 6H-SiC sample became Si rich, although we do not have sufficient information to establish the correlation between the conversion efficiency enhancement and the Si enrichment on the surface.

It should be noted that for both n-type 4H-SiC and 6H-SiC material, the conversion efficiency is $\sim 1 \times 10^{-4}$. This relatively high value confirms the practical value of using SiC as a primary moderator and suggests a high value of y_0, which can indeed be calculated from equation (1). Brusa *et al* [25] estimated that the geometry factor for a side-mounted annular ^{22}Na source is ∼0.3. The mean implant depth was found to be $R \sim 80$ μm by using the implantation profile $P(x) = \alpha \exp(-\alpha x)$ with the stopping coefficient α given by two different equations: $\alpha = 2.8\rho Z^{0.15}\bar{E}^{-1.19}$ [26] and $\alpha = 16\rho E_m^{-1.43}$ [27], where ρ is the density, Z is the mass number, $\bar{E}$ and E_m are the mean energy and the maximum energy for implanting β^+-particles. Taking the positron diffusion length for SiC to be $L_+ \sim 60$ nm, the branching ratio for positron emission from the surface was found to be $y_0 \sim 44\%$, which is close to the value of Störmer *et al* [7] (∼40%) and a bit higher than that obtained by Jørgensen *et al* [8] (∼30%).

In order to find the positron work functions of the as-grown and 650 and 1000 °C annealed n-type 6H-SiC samples, their integral spectra (with maximum counts normalized to unity) are plotted against $V_R - V_0$ in figure 3(a). The 1400 °C annealed sample was excluded because the count of slow positrons emitted was too low to obtain a reasonably accurate estimation of

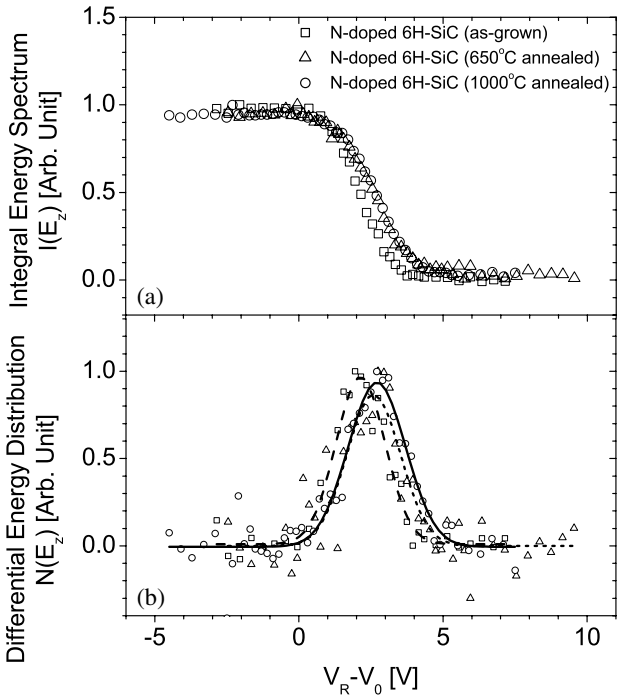

Figure 3. (a) Integral energy spectra of the as-grown, the 650 °C annealed, and the 1000 °C annealed n-type 6H-SiC. (b) Energy distributions of the positrons re-emitted from the surface of the as-grown, the 650 °C annealed, and the 1000 °C annealed n-type 6H-SiC, which are the derivatives of the integral emission spectra shown in (a). The dashed curve, the dotted curve, and the solid curve are the Gaussian curves fitted to the data for the as-grown, the 650 °C annealed, and the 1000 °C annealed n-type 6H-SiC respectively.

its work function. From figure 3(a), the integral spectra with higher annealing temperatures shift slightly to the higher-energy side, which implies a slight increase of the positron work function ϕ_+ with increasing annealing temperature. The energy distributions of the positrons emitted from these surfaces were fitted with Gaussian functions and the resulting curves are shown in figure 3. The χ^2-values of the Gaussian fits are all reasonably good and are given in table 1. From the Gaussian peak positions, the work functions ϕ_+ of the three samples were found, and these are tabulated in table 1. Consistent with the visual observation of the shifts of the integral spectra with increasing annealing temperature, the positron work functions of the as-grown, the 650 °C annealed, and the 1000 °C annealed n-type 6H-SiC samples were found to be -2.2 ± 0.5, -2.6 ± 0.3, and -2.7 ± 0.3 eV respectively.

Störmer *et al* [7] have studied positron emission from the surfaces of untreated n-type 6H-SiC ([0001] orientation and Si surface). By implanting slow positrons from a positron beam, the number of emitted positrons was measured as a function of the retarding potential of a RFA with the use of a collimated HPGe detector. The positron work function of this untreated sample was found to be -3.0 ± 0.2 eV. Kuriplach *et al* [28] have analysed the same data set with consideration of the epithermal positron contribution. Nangia *et al* [9] have performed positron emission measurements on the same sample as Störmer *et al* [7] used, and another similar 6H-SiC sample, by directly detecting the emitted positrons with a micro-channel plate (MCP). The re-analysis carried out by Kuriplach *et al* [28] and the results obtained for the two samples in the Nangia *et al* [9] study gave a consistent result of

$\phi_+ = -2.1 \pm 0.1$ eV, which is also close to the value of -2.2 eV obtained in the present study (though the surface orientation is not the same). In the theoretical work of Kuriplach *et al* [28], the linear muffin-tin orbital (LMTO) method was used to calculate the positron affinity A_+ of silicon carbides. In treating the positron correlation potential, different approaches have been attempted. The experimental positron affinity was deduced by the measured values of the positron work function and electron work function $\phi_- + \phi_+ + A_+ = 0$. The theoretical values for 4H-SiC and 6H-SiC were found to be independent of the polytype but varied from -4.7 eV (insulator model, IM) to -8.5 eV (rare-gas-solid model, RGSM) depending on the treatment of the positron correlation potential. With our present value of the positron work function of ~ -2.2 eV (which is also very close to that obtained by Kuriplach *et al* [28] and the electron work function value of $\sim$6.4 eV), our present result corresponds to a positron affinity of $A_+ = -4.2$ eV, which is not far away from the IM-predicted value but significantly differs from those predicted using the other models. However, Kuriplach *et al* [28] have pointed out there is at present no positron correlation potential model giving a consistently good prediction of positronic parameters. It should be noted that while the IM gives a positron affinity value relatively close to the measured one, its predicted positron lifetime value deviates significantly from the experimental one.

Slow-positron emission from as-grown Al-doped p-type 4H-SiC and 6H-SiC materials was also observed, but the conversion efficiency was found to be only $\sim 10^{-5}$, some ten times less than those of the n-type SiC materials. Defects in as-grown p-type 6H-SiC with a similar p concentration to the present sample have been studied by the positron lifetime technique [29]. It was found that the only positron trapping centre was the $V_C V_{Si}$ divacancy with a concentration of about 4×10^{16} cm^{-3}. Positron lifetime studies have been carried out on as-grown n-type 6H-SiC (also with an n concentration similar to that of the n-type 6H-SiC sample used in the present study) [22, 29]. V_C, V_{Si}, $V_C V_{Si}$, and positron shallow traps were identified as positron trapping centres in this as-grown n-type material, and the concentration of the $V_C V_{Si}$ divacancy was found to be about 8×10^{16} cm^{-3}, which is slightly higher than that for the p-type material. Comparing the as-grown p-type material with the n-type 6H-SiC materials, it was shown in [29] that fewer positrons are trapped by vacancy-type defects for the case of p-type material. This implies that the small conversion efficiency for the p-type material is not due to positron trapping in the bulk, but is most probably due to a surface process. Adverse surface band bending is the most likely cause of low positron emission at p-type material surfaces. Any mid-gap surface electronic states will tend to cause the loss of electrons to the bulk and, when this occurs, a strong electric field is set up, pulling positrons into the crystal. For the p-type 6H-SiC sample, the effect of annealing was also investigated and the results are also given in table 1. Unlike the case for the n-type 6H-SiC where the efficiency was enhanced by the 1000 °C annealing, the efficiency of p-type 6H-SiC remained consistently low: $\sim 10^{-5}$ after the 1000 °C annealing. The positron work function for the p-type SiC materials was not found because of the poor statistics of the integral positron count spectra.

4. Conclusions

In the present work, positron emission measurements have been performed on n-type 4H-SiC, n-type 6H-SiC, p-type 4H-SiC, and p-type 6H-SiC. The positron work functions of the n-type as-grown 4H-SiC and 6H-SiC have been found to be -2.3 and -2.2 eV respectively. The magnitude of the positron work function of the n-type 6H-SiC sample was found to increase to 2.7 eV upon 1000 °C annealing. The positron conversion efficiency for the as-grown n-type materials ($\sim 10^{-4}$) is an order of magnitude higher than that for the p-type ones ($\sim 10^{-5}$). This has been attributed to the band bending at the surface of p-type materials, which inhibits

positron diffusion to the emitting surface. For the n-type 6H-SiC material, the conversion efficiency was observed to increase by 75% upon 1000 °C annealing but was found to decrease by an order of magnitude upon further 1400 °C annealing. The conversion efficiency ε of the n-type Lely-grown SiC bulk material is as high as that of the well annealed tungsten moderator, and it can be further increased by using epitaxial material which has a much longer positron diffusion length. The present results show that SiC is a very attractive material for use in primary moderation and secondary re-moderation, as it has a high conversion efficiency and does not require any pre-treatment, e.g. 2000 °C annealing (as is required for a W moderator).

Acknowledgments

The work described in this paper was partially supported by grants from the Research Grant Council of the Hong Kong Special Administrative Region, China (under project nos HKU7113/98P and HKU7137/99P), and the HKU CRCG. We would also like to offer sincere thanks to I P Hui and K L Chan for their work on the AES measurements, and also to M H Xie for fruitful discussion.

References

[1] Schultz P J and Lynn K G 1988 *Rev. Mod. Phys.* **60** 701
[2] Coleman P G (ed) 2000 *Positron Beams and their Applications* (Singapore: World Scientific)
[3] Cherry W 1958 *PhD Thesis* Princeton University, NJ
[4] Gullikson E M and Mills A P Jr 1986 *Phys. Rev. Lett.* **57** 376
[5] Suzuki R *et al* 1998 *Japan. J. Appl. Phys.* **37** 4636
[6] Weng H M, Ling C C, Hui I P, Beling C D and Fung S 2001 *Appl. Surf. Sci.* at press (presented in *SLOPOS-9*)
[7] Störmer J, Goodyear A, Anwand W, Brauer G, Coleman P G and Triftshäuser W 1996 *J. Phys.: Condens. Matter* **8** L89
[8] Jørgensen L V, van Veen A and Schut H 1996 *Nucl. Instrum. Methods* B **119** 487
[9] Nangia A, Kim J H, Weiss A H and Brauer G 2002 *J. Appl. Phys.* **91** 2818
[10] Brandes G R, Mills A Jr and Zuckerman D 1992 *Mater. Sci. Forum* **108** 1362
[11] Lynn K G and McKee B T A 1979 *Appl. Phys.* **19** 247
[12] Merrison J P, Charlton M, Deutch B I and Jørgensen L V 1992 *J. Phys.: Condens. Matter* **4** L207
[13] Beling C D, Simpson R I, Charlton M, Jacobsen F M and Griffith T C 1987 *Appl. Phys.* A **42** 111
[14] Shan Y Y, Au H L, Ling C C, Lee T C, Panda B K, Fung S, Beling C D, Wang Y Y and Weng H M 1994 *Appl. Phys.* A **59** 259
[15] Beling C D, Fung S, Li Ming, Gong M and Panda B K 1999 *Appl. Surf. Sci.* **149** 253
[16] Nangia A, Kim J H, Weiss A H and Brauer G 1997 *Mater. Sci. Froum* **255–7** 711
[17] Hu Y F, Lam C H, Ling C C, Fung S, Beling C D and Weng H M 2001 *Mater. Sci. Forum* **363–5** 120
[18] Brauer G, Anwand W, Coleman P G, Störmer J, Plazaola F, Campillo J M, Pacaud Y and Skorupa W 1998 *J. Phys.: Condens. Matter* **10** 1147
[19] Anwand W, Brauer G, Wirth H, Skorupa W and Coleman P G 2001 *Appl. Surf. Sci.* at press (presented in *SLOPOS-9*)
[20] Britton D T, Barthe M F, Corbel C, Desgardin P, Egger W, Sperr P, Kögel G and Triftshäuser W 2001 *Appl. Surf. Sci.* at press (presented in *SLOPOS-9*)
[21] Morkoc H, Strite S, Gao G B, Lin M E, Sverdlov B and Burns M 1994 *J. Appl. Phys.* **76** 1363
[22] Ling C C, Beling C D and Fung S 2000 *Phys. Rev.* B **62** 8016
[23] Murray C A and Mills A P Jr 1980 *Solid State Commun.* **34** 789
[24] Jibaly M, Weiss A, Koyman A R, Mehl D, Stiborek L and Lei C 1991 *Phys. Rev.* B **44** 12 166
[25] Brusa R S, Grisenti R, Oss S, Zecca A and Dupasquier A 1985 *Rev. Sci. Instrum.* **56** 1531
[26] Mourino M, Löbl H and Paulin R 1979 *Phys. Lett.* A **71** 106
[27] Brandt W and Paulin R 1977 *Phys. Rev.* B **15** 2511
[28] Kuriplach J, Šob M, Brauer G, Anwand W, Nicht E-M, Coleman P G and Wagner N 1999 *Phys. Rev.* B **59** 1948
[29] Ling C C, Deng A H, Fung S and Beling C D 2000 *Appl. Phys.* A **70** 33